Eurasian ChemTech Journal 5 (2003) 127-135

State of the Active Component and Catalytic Properties of Pd/C Catalysts on the Selective Hydrogenation of Butadiene-1,3 into Butylenes

V.V. Chesnokov*, I.P. Prosvirin, V.I. Zaikovskii and N.A.Zaitseva

Boreskov Institute of Catalysis, Prosp. Akad. Boreskova, 5, 630090 Novosibirsk, Russia

Abstract

Palladium (0.25-5.8 wt.%) was supported on three different types of filamentous carbon in which the basal graphite planes are arranged along, crosswise and at a 45° angle to the axis of a nanofiber. HREM, XPS and X-ray techniques were used to study the state of high dispersed Pd particles supported on the filamentous carbon. It was established that the type of the carbon support affects the properties of the active component. The high disperse Pd particles most strongly interact with the prismatic planes of graphite to provide electron transfer from palladium to the support, which stabilizes palladium in a more dispersed state. Because of this strong interaction, Pd^{2+} is stabilized in the ionic state. A change in the properties of the palladium particles initiates changes in the catalytic properties of Pd/C catalysts in the reaction of selective hydrogenation of 1,3-butadiene into butylenes. An increase in the fraction of Pd^{2+} in the catalyst composition results in the decrease of both total activity and selectivity of Pd/C catalysts in the considered reaction.

Introduction

Palladium catalysts supported on the metal oxides [1-5] exhibit the highest activity in the reactions of hydrogenation. However, carbon supports have a number of advantages over oxide metal supports. The properties of Pd/C catalysts were studied in a number of works [6-9]. It was found that hydrogenation is a structurally sensitive reaction, i.e. its activity and selectivity depend primarily on the size and face type of the catalytically active metal particles [9,10]. When the chemical composition of the surface is unchanged, the size of the metal particles determines the electronic structure of the active sites, the nature of interaction between the reagents, and catalytic properties of the system.

In addition, the metal-carbon support interaction can also affect the metal state. This effect depends, in turn, on the graphite edges that emerge the surface. Since carbon supports have a rather complex structure and the possibility to synthesize a support with the specified properties is limited, the effect of this interaction on the catalytic properties of Pd/C catalysts has not been adequately investigated. In the present work we studied the effect of different graphite edges emerging the filamentous carbon surface on the state of palladium and catalytic properties of the Pd/C catalysts in the selective hydrogenation of butadiene-1,3 into butylenes. We used filamentous carbon as a subject of this study, because a considerable progress has been achieved in the understanding of its formation mechanism and control of its crystallographic structure. In our earlier study [11] we have reported the preparation of three different types of filamentous carbon in which the basal graphite planes are arranged along, crosswise and at a 45° angle to the filament axis, *i.e.* coaxial-cylinder, stack-like and coaxial-conic arrangement of carbon filaments.

*corresponding author. E-mail: Chesn@catalysis.nsk.su

Experimental

Carbon filaments were prepared from hydrocarbons such as CH_4 and C_4H_6 over the Ni-containing catalysts in a quartz flow reactor supplied with a Mac-Ben balance under gradientless conditions with respect to temperature. The preparation methods of filamentous carbon with different orientations of graphite layers in the fiber body are described in detail elsewhere [11].

X-ray diffraction (XRD) patterns of the samples were recorded on a Siemens D-500 diffractometer using CuK_α radiation (a graphite monochromator on

the reflected beam).

The carbon filaments and supported palladium particles were studied by high-resolution transmission electron microscopy and electron diffraction using a JEM-2010 FX instrument.

The dispersion of the Pd/C catalysts was determined by chemisorption of CO at 20°C using the pulse techniques described in [12].

Since the catalysts used for growing of carbon filaments contain metallic nickel or nickel-copper alloys, the resulting products also contain nickel (0.5 - 15 wt.%). To determine the concentration of nickel, a VRA-20 analyzer supplied with a W anode in the X-ray tube was used to perform X-ray spectral analysis of the carbon filaments.

Both the carbon supports and Pd/C catalysts were studied by XPS using a VG ESCALAB HP photoelectron spectrometer with non-monochromatic radiation AlK_α ($h\nu$ = 1486.6 eV, 200 W). During spectra recording, the pressure of residual gases in the analyzer chamber was 5×10^{-7} Pa.

The binding energy (E_b) scale of the spectrometer was preliminary calibrated using the peaks of Au $4f_{7/2}$ (84.00 eV) and Cu $2p_{3/2}$ (932.67 eV) core levels. To prevent charging effects resulting from photoemission during deposition of the conducting samples on the non-conducting support, the samples were rubbed into a nickel net. The samples were loaded into the spectrometer in air. As an internal standard we used a line of carbon (C 1s, E_b = 284.4 eV) of the support material.

The relative concentrations of the elements occurring on the catalyst surface and the ratios of their atomic percentage were determined from integral intensities of the photoelectron lines related to the corresponding atomic sensitivity coefficients [13].

The reaction of butadiene hydrogenation was performed in a flow-circulating setup at 60-150°C. The catalyst sample amount was 0.05 g, the rates of hydrogen and unsaturated hydrocarbon flows were 7 and 1.4 l/h, respectively. The reaction products were analyzed by chromatography. As adsorbents we used zeolite NaX and triethylene glycol n-butyrate on diatomaceous earth.

To develop methods for the controlled manufacturing of graphite filaments with coaxial-cylinder, stacking and coaxial-conic arrangements of graphite basal layers in the nanofiber, we used data on the formation of graphite phases from carbon atoms resulting from the hydrocarbon decomposition (the carbide cycle mechanism) over the iron sub-group metals (Fig. 1), since filamentous carbon is a metal-carbon system. In order to prepare a "pure" carbon material, a solution of nitrohydrochloric acid was used for etching the metal particles that catalyze the growth of filamentous carbon. Unfortunately, the boiling of carbon filaments in nitrohydrochloric acid for several hours does not completely etch nickel from the samples, because some metal atoms are interlocked by carbon. Table 1 shows the concentration of nickel in carbon nanofibers after etching.

The fact that nickel metal is interlocked by carbon is confirmed by electron microscopy and studies on the catalytic activity of carbon nanofibers on the butadiene-1,3 hydrogenation. As follows from these studies, carbon nanofibers are not catalytically active in this reaction in a temperature range of 60-150°C.

After etching, three types of carbon filaments were covered by palladium from aqueous solutions of $PdCl_2$. Data on the palladium concentration in the samples are given in Table 2.

HREM, XPS and X-ray techniques were used to study the state of high disperse palladium particles supported on the carbon filaments.

Results and Discussion

Study of Pd/C catalysts by X-ray diffraction

The X-ray diffraction method shows that the car-

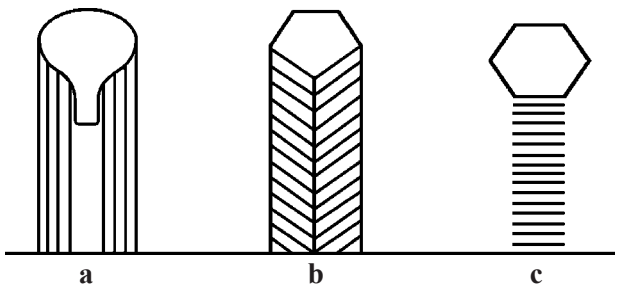

Fig. 1. Schematic representation of the longitudinal section of the main types of carbon filaments. Spatial arrangement of the basal graphite planes: (a) coaxial-cylinder, (b) coaxial-conic and (c) stack-like.

Table 1

Concentration of nickel in the carbon fibers after etching with a nitrohydrochloric acid solution

Type of carbon nanofibers	Concentration of Ni, wt.%
Stack-like	0.5
Coaxial-conic	0.9
Coaxial-cylinder	6.1

Table 2
Concentration of palladium in catalysts Pd/C

Sample number	Type of filamentous carbon structure	Concentration of Pd, wt.%
1	Stack-like	0
2	Stack-like	0.25
3	Stack-like	0.5
4	Stack-like	2.5
5	Stack-like	5.8
6	Coaxial-conic	0.58
7	Coaxial-conic	3.15
8	Coaxial-cylinder	0.25
9	Coaxial-cylinder	0.60
10	Coaxial-cylinder	2.62

bon fibers are formed by graphite layers ordered to a variable extent. The X-ray patterns (not shown) exhibit an intense line of graphite at $2\Theta = 26°$. XRD analysis does not reveal nickel metal in the fiber samples with coaxial-conic and stacking structures after their treatment with a nitrohydrochloric acid solution. For the carbon filament sample with a coaxial-cylinder structure, the X-ray patterns exhibit weak lines typical of Ni (Table 3).

As the carbon supports with both coaxial-cylinder and coaxial-conic structures were impregnated with an aqueous solution of $PdCl_2$ and dried at 100°C, the lattice parameters of graphite did not change. These parameters maintain when the Pd/C catalysts are reduced at 250°C. When the filamentous carbon sample with a stack-like structure is impregnated with an aqueous solution of $PdCl_2$ and dried at 100°C, the graphite lattice parameter increases by 0.1 Å irrespective of the amount of the supported palladium. As the Pd/C samples are reduced at 250°C, the lattice parameter decreases to its initial value. These data suggest that either the solvent or Pd^{2+} and Cl^- ions can easily penetrate into the interlayer space of the graphite composed of stack-like nanofibers, but are pushed back to the surface after reduction.

Study of Pd/C catalysts by XPS

The chemical compositions of the Pd/C catalysts were determined by XPS. The chemical shifts of the core levels were correlated, which makes it possible to suggest the presence of chemical compounds and to determine the degree of palladium oxidation.

All studied samples exhibit the presence of chlorine, carbon, oxygen and palladium. No additional admixtures were registered within the accuracy of the XPS method. This method provides information on the state of the surface layer with a depth range of 25-30 Å. The fact that nickel was not registered by the XPS method proves the supposition that nickel particles were blocked by carbon.

It should be noted that the intensity of the Pd 3d line is very weak in the spectra of the sample containing 0.5 wt.% palladium, that is why the Pd 3d spectrum was accumulated during a long period of time.

Figure 2 shows the C 1s spectra of the Pd/C samples prepared from carbon nanofibers with a stack-like structure. The stack-like structure of filamentous carbon can be presented as a large number of basal graphite plates arranged as a book pile. Only prismatic graphite edges are exposed on the external nanofilamentous surface. Because of the extremely high level of bond unsaturation of the carbon atoms at the prismatic planes, the carbon platelets bind between themselves [14].

The analysis of the above spectra shows that the C 1s peak with a binding energy of 284.4 eV (the half-width of the peak is about 1.5-1.55 eV) is typical for all studied samples. The shape of the C 1s peak is slightly asymmetric: there is a shoulder at higher binding energies, which can be associated with the presence of C-Cl and C-O bonds on the carbon support surface. The intensity of the carbon peak insignificantly changed in the investigated samples.

Table 3
Properties of filamentous carbon according to XRD analysis

Carbon nanofibers	Temperature of production of nanofibers, °C	Parameters of graphite lattice, Å	Region of coherent scattering, Å
Coaxial-conic	500	3.44	50
Stack-like	600	3.40	65
Coaxial-cylinder	750	3.39	140

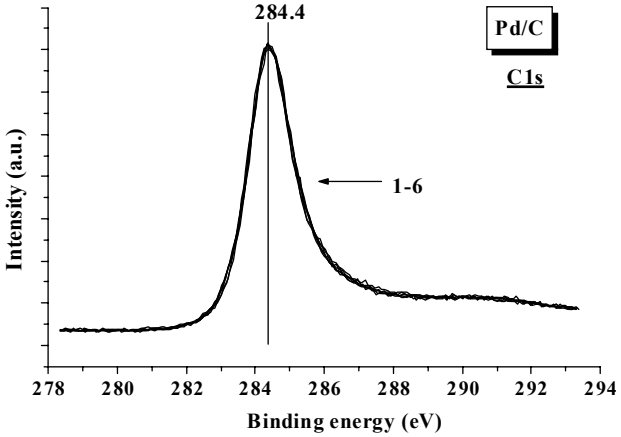

Fig. 2. Spectra C 1s of the filamentous carbon samples with a stacking structure (1) and catalysts Pd/C (2-6) prepared by depositing palladium on the carbon nanofibers with a stack-like structure.
2: 0.5 wt.% Pd/C after drying at 100°C;
3: 0.5 wt.% Pd/C after reduction at 250°C;
4: 0.5 wt.% Pd/C after reduction at 300°C;
5: 2.5 wt.% Pd/C after reduction at 250°C;
6: 5.8 wt.% Pd/C after reduction at 250°C.

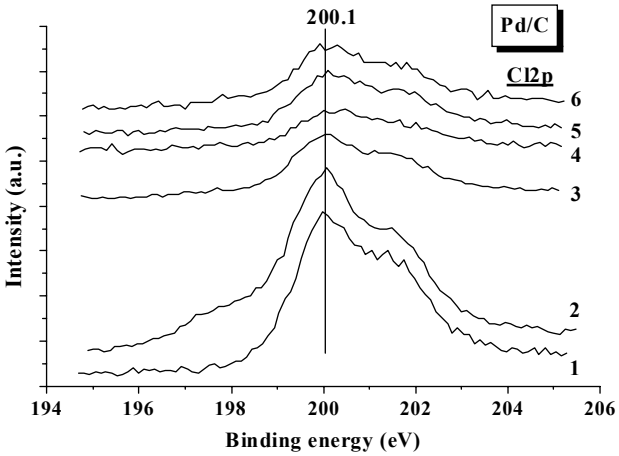

Fig. 3. Spectra C 12p of carbon nanofibers with a stack-like structure (1) and catalysts Pd/C (2-6) prepared by deposition of palladium on the carbon nanofibers with a stack-like structure.
2: 0.5 wt.% Pd/C after drying at 100°C;
3: 0.5 wt.% Pd/C after reduction at 250°C;
4: 0.5 wt.% Pd/C after reduction at 300°C;
5: 2.5 wt.% Pd/C after reduction at 250°C;
6: 5.8 wt.% Pd/C after reduction at 250°C.

Thus, the C 1s peak can solely be attributed to the carbon support.

The Cl 2p spectra are shown in Fig. 3. The binding energy of the C1 2p line is almost similar for all samples and equals 200.1 eV. The line with a peak maximum at 200.1 eV can be attributed to chlorine atoms which are bound to the support carbon. Close intensities of the chlorine peaks were obtained for the samples with a stacked structure and the 0.5 wt.% Pd/C sample prepared by depositing $PdCl_2$ on the carbon filaments with a stacked structure after drying at 100°C. For the latter sample, there is a shoulder at lower binding energies with a peak maximum at 198.0-198.4 eV which can be attributed to α-$PdCl_2$ [15]. Note that the Cl/C ratio of this sample prepared by depositing of $PdCl_2$ and drying is higher than that of carbon nanofibers with a stack-like arrangement (see Table 4).

During further reduction of the 0.5 wt.% Pd/C sample (stacking arrangement) with hydrogen at 250 and 300°C, the Cl/C ratio decreases by a factor of 3.3 and 5 as compared to the 0.5 wt.% Pd/C sample (stacking arrangement) after its drying. Reducing of palladium chloride results in metallic palladium. Figure 4 presents the Pd 3d photoelectron spectra.

After drying, the Pd 3d spectrum of the 0.5 wt.% Pd/C sample (stack-like arrangement) exhibits two palladium states: the main peak with a binding energy of 337.5 eV and a shoulder (336.4 eV) in the

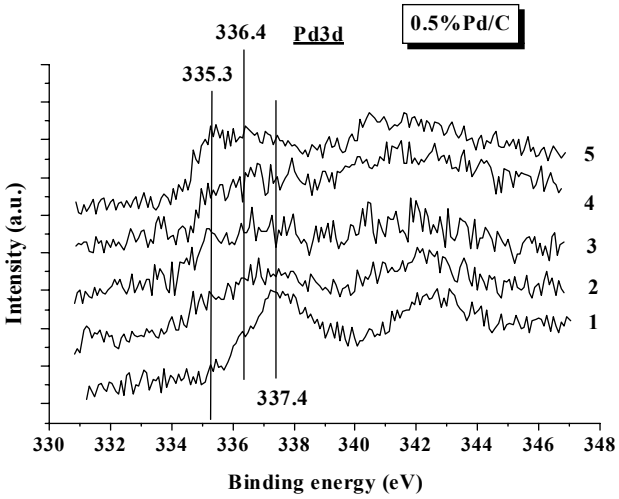

Fig. 4. Spectra Pd3d of catalyst 0.5% Pd/C (stack-like structure):
1: after drying at 100°C;
2: after reduction at 250°C;
3: after reduction at 300°C;
4: after reduction at 250°C and subsequent calcination at 450°C;
5: after reduction at 250°C and subsequent calcination at 650°C.

region of lower binding energies. Based on the fact that the binding energy of the main peak (337.5 eV) is close to that of the palladium-chlorine complexes and taking into account the fact that the sample exhibits the shoulder in the region of low binding ener-

Table 4
Ratio of atomic concentrations of elements in samples Pd/C

Type of carbon filaments	Pd Wt.%	T_{red}, °C	Pd/C	Pd/Cl	Pd/O	O/C	Cl/C
Stack-like	0					0.054	0.025
Stack-like	0.5	unreduced	0.0014	0.034	0.020	0.055	0.037
Stack-like	0.5	250	0.0012	0.11	0.024	0.049	0.011
Stack-like	0.5	300	0.0012	0.18	0.028	0.044	0.0069
Stack-like	0.5	250 / $T_{calcination}$ / 450	0.0011	0.23	0.031	0.037	0.0051
Stack-like	0.5	250 / $T_{calcination}$ / 650	0.0013	0.82	0.046	0.029	0.0016
Stack-like	2.5	250	0.0038	0.31	0.066	0.056	0.012
Stack-like	5.8	250	0.0088	0.7	0.1	0.085	0.012
Coaxial-cylinder	0.60	unreduced	0.0019	0.083	0.018	0.11	0.024
Coaxial-cylinder	0.60	250	0.0024	0.83	0.068	0.036	0.0028
Coaxial-conic	0.58	unreduced	0.0027	0.087	0.029	0.082	0.027
Coaxial-conic	0.58	250	0.0011	0.21	0.031	0.052	0.007

gies for the C1 2p line (198.2-198.5 eV) corresponding to chlorine in $PdCl_2$, one can attribute this peak to $PdCl_2$ presented on the sample surface after its impregnation and drying. As follows from the literature data, the binding energy of metallic palladium, Pd^o, is 335.3 eV. For small clusters (<20-30 Å), the binding energy of the core level shifts and the valence band narrows with respect to the bulk metal [16-20]. As the number of atoms in the cluster decreases, E_b of the core levels increases. For highly dispersed Pd/C catalysts, the shift in the binding energy of the core level is 1.0-1.3 eV. For this reason, the shoulder with a binding energy of 336.4 eV belongs to the particles of high dispersed palladium, Pd^+, that is the electrons are transferred from palladium to the carbon support.

As the 0.5 wt.% Pd/C samples were subsequently reduced in a hydrogen flow at 250 and 300°C, the peak with a binding energy of 337.5 eV decreased and the peak with a binding energy of 336.4 eV (typical for Pd^+) increased. Note that the intensity of the Cl 2p line of the sample reduced at 300°C slightly decreases as compared to the sample reduced at 250°C. In addition, the spectrum exhibits a small shoulder with a binding energy of 335.3 eV which is typical of palladium metal observed in the sample reduced at 300°C. The fact that the intensity of the palladium peak in the reduced samples is lower than that in the unreduced samples suggests that the process of reduction is accompanied by intercalation of palladium atoms into the interlayer space of graphite by sintering of palladium particles into larger particles as compared to the initial $PdCl_2$/C sample (stack-like arrangement) obtained after drying. It should be noted that after reduction some part of palladium with a binding energy of 337.5 eV remains due to a stronger interaction between a part of palladium chloride and the support. It is reasonable to suggest that Pd^{2+} ions are incorporated between basal planes of graphite.

XRD does not confirm this suggestion, because its sensitivity is not sufficient. According to the XPS method, a drop in the Pd concentration is about 20% of its concentration (0.5 wt.%), that is, 0.1 wt.% of palladium intercalates into graphite. Only a small amount of palladium intercalates into filamentous

carbon. This observation suggests that the intercalation of palladium proceeds with difficulty and between the layers that have the largest interplanar spacing.

Heating of the reduced 0.5 wt.% Pd/C samples (stack-like arrangement) at 450 or 650°C for 1 h does not result in a significant sintering of palladium, but the palladium states are redistributed (Fig. 5). To accurately determine the ratio between metallic and oxidized palladium, we deconvolved the complex photoelectron spectra into individual peaks (FitXPS program). It is evident that the amount of metallic palladium Pd^o increases and that of Pd^{2+} decreases. This thermal stability of the Pd/C catalysts suggests a strong interaction between palladium and the support. Note that the Pd 3d/C 1s ratio increases consequently the amount of palladium on the carbon surface by ~10-20% after heating at 650°C. This observation can be attributed to an egress of the intercalated palladium from the support volume, size redistribution of the supported Pd^0 particles and spreading of the smaller particles over the support. The relations between the atomic concentrations of the elements in the considered samples are given in Table 4.

According to the experimental data, the carbon filaments with a stack-like structure exhibit stronger adsorption properties compared to the nanofibers with coaxial-conic and coaxial-cylinder structures. Thus, after etching with a nitrohydrochloric acid solution, the surface of all types of carbon filaments exhibits significant amounts of chlorine atoms (Table 4). XPS data show that the processes of deposition of palladium chloride and reduction with hydrogen at 250°C provide different changes in the concentration of chlorine atoms on the filaments. In the filamentous carbon with a coaxial-cylinder structure, chlorine is not observed. The concentration of chlorine in the filamentous carbon with a stack-like structure only slightly decreases (by a factor of 3-4).

To provide a distinct identification of palladium states, one should use the Pd/C catalysts (with a stack-like arrangement) containing 2.5 and 5.8 wt.% of palladium (Fig. 6). The analysis of the Pd 3d spectra suggests that after reduction at 250°C, palladium exists as metallic Pd^o (335.3 eV) and oxidized Pd^+ (336.4 eV) states. Note that the fraction of metallic palladium is higher in the second sample. This result agrees well with the data on the palladium dispersion. As the concentration of palladium increases from 0.5 to 5.8 wt.%, the dispersion of palladium decreases from 33 to 50 Å (see Table 5).

From the above types of filaments, the filamentous carbon with a stack-like arrangement is characterized by stronger interaction with palladium which manifests itself as a more pronounced redistribution of electron density in the palladium/carbon system and higher dispersion of Pd. In the Pd3d spectrum, the peak belonging to metallic palladium (335.3 eV) shifts to higher energies typical of the oxidized palladium (336.4 eV), which suggests a transfer of electrons from palladium to carbon.

Study of Pd/C catalysts by high-resolution transmission electron microscopy

The high-resolution transmission electron micros-

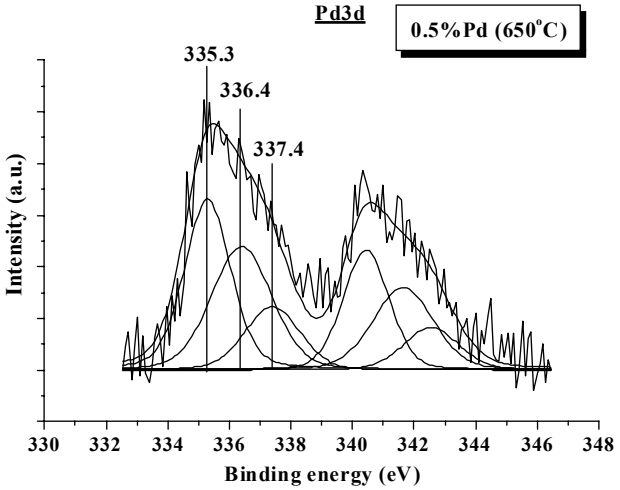

Fig. 5. Spectrum Pd3d of catalyst 0.5 wt.% Pd/C (stack-like), exposed to reduction at 250°C and subsequent heating at 650°C, is resolved into separate spectral components.

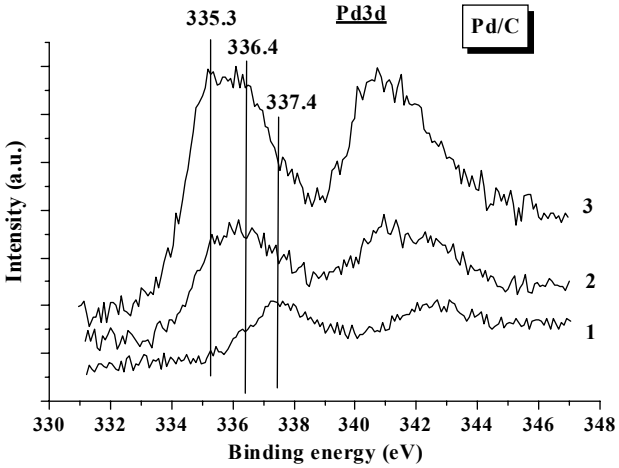

Fig. 6. Spectra Pd3d of both catalyst 0.5 wt.% Pd/C (stack-like) after drying (1) and reduced catalysts 2.5% Pd/C (stack-like) (2) and 5.8% Pd/C (stack-like) (3).

Table 5
Effect of properties of carbon supports on dispersion of catalysts Pd/C

Type of filamentous carbon	Concentration of Pd	T_{red}	Dispersion
Stack-like	0	250	-
Stack-like	0.5	250	30
Stack-like	0.5	250 ($T_{calcination.}$=450)	70
Stack-like	0.5	250 ($T_{calcination.}$=650)	70
Stack-like	2.5	250	31
Stack-like	5.8	250	50
Coaxial-conic	0.58	250	31
Coaxial-conic	3.15	250	73
Coaxial-cylinder	0.60	250	41
Coaxial-cylinder	2.62	250	70

copy examination of the Pd/C catalysts, prepared by depositing of ~0.5 wt.% Pd on the filamentous carbon, does not reveal the existence of palladium particles. This observation suggests that palladium particles are highly dispersed. Only the micrographs of the 0.5 wt.% Pd/C catalyst (filamentous carbon with a stack-like structure) heated at 450°C in inert medium exhibit particles 5-10 Å in size that have a higher contrast than graphite (see Fig. 7). This indicates that the catalyst contains highly disperse palladium particles of 5-10 Å. As the concentration of palladium in the Pd/C catalyst increases to 2 wt.%, dispersion of palladium particles decreases. According to the micrographs of the palladium particles supported on the filaments with coaxial-cylinder and coaxial-conic structures (Figs. 8, 9), the size of palladium particles is in a range of 20-50 Å. The most dispersed palladium particles are observed on the filamentous carbon with a stack-like structure.

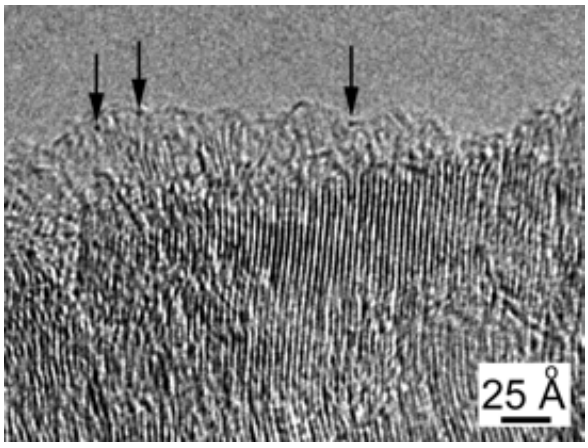

Fig. 7. Electron micrograph of catalyst 0.5 wt.% Pd/C, supported on the filamentous carbon with a stack-like structure, heated at 450°C in the inert gas.

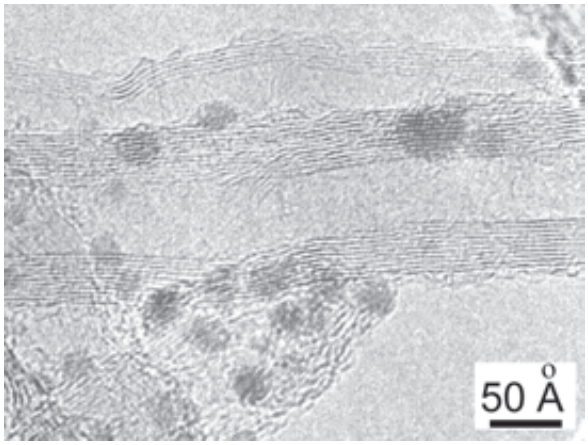

Fig. 8. Electron micrograph of catalyst 2 wt.% Pd/C supported on the filamentous carbon with a coaxial-cylinder structure.

Catalytic Measurements

Activity and selectivity of the Pd/C catalysts in the selective hydrogenation of butadiene-1,3 were determined in the temperature range 60-150°C. Specific activity of the catalysts slightly increases with increasing temperature, which indicates that the activation energy of this reaction is not high. Table 6 shows the catalytic activity of different Pd/C catalysts determined at 100°C. The Pd/C catalysts supported on the filamentous carbon with a coaxial-cylinder structure exhibit the highest activity. We attribute this observation to lower activity of Pd^{2+} as

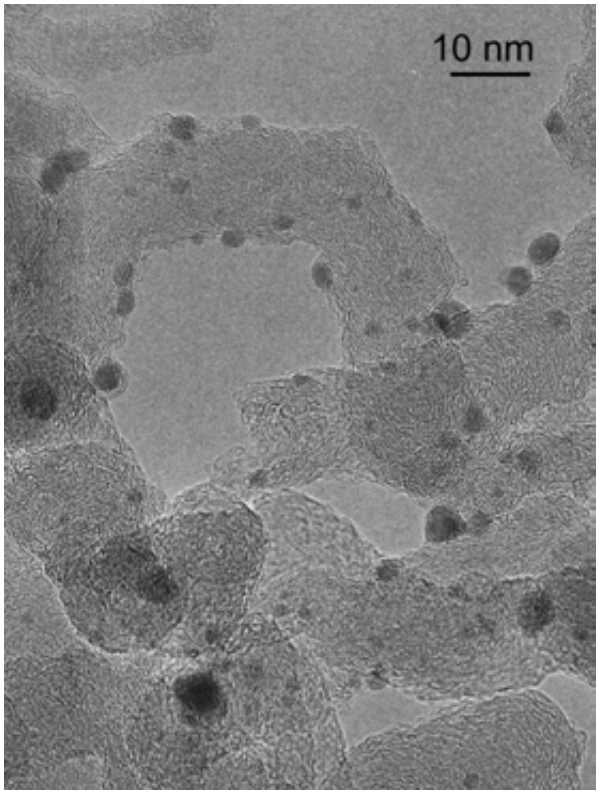

Fig. 9. Electron micrograph of catalyst 2 wt.% Pd/C supported on the filamentous carbon with a coaxial-conic structure.

compared to Pd^+ and Pd^o and probably to intercalation of some palladium into the volume of filamentous carbon. Since the concentration of Pd^{2+} in the 0.5 wt.% Pd/C sample (stack-like structure) is higher than that in both 0.58 wt.% Pd/C (coaxial-conic structure) and 0.6 wt.% Pd/C samples (coaxial-cylinder), the activity of this sample is lower.

The reaction products of the butadiene hydrogenation are butane, 1-butene, cis- and trans-2-butenes. The relations between butenes varies only insignificantly. The amounts of 1-butene and cis-2-butene are almost the same, whereas the amount of trans-butene exceeds that of 1-butene by a factor of 1.5-2.0

Figure 10 shows the effect of the carbon support on the selectivity of the Pd/C catalysts with respect to butenes in the butadiene hydrogenation. Interestingly, the selectivity curves with respect to butenes vs. the concentration of palladium go through a maximum for the samples with both coaxial-cylinder and stack-like structures. As the concentration of palladium decreases from 5.8 to 0.5 wt.%, the selectivity of the Pd/C catalyst increases. Therefore, an increase in the dispersion of metallic palladium particles provides an increase in the reaction selectivity to butenes. However, as the palladium concentration decreases from 0.5 to 0.25 wt.%, the reaction selectivity decreases. We attribute this observation to an increase in the concentration of ionic palladium. Consequently, Pd^{2+} exhibits both low activity and selectivity in the reaction of selective hydrogenation of 1,3-butadiene into butylenes.

This suggestion was additionally confirmed by catalytic data which were not presented in this paper. As the concentration of Pd decreases in the sample (stacking arrangement) below 0.1 wt.%, the activity of the Pd/C catalyst in the selective hydrogenation of 1,3-butadiene into butylenes becomes zero, whereas 0.1 wt.% Pd/C (supported on the filamentous carbon of the other structure) show high activity even at room temperature.

Acknowledgement

The authors are grateful for financial supply of

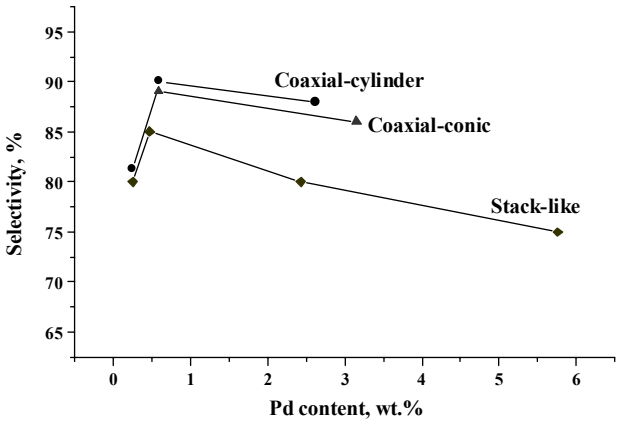

Fig. 10. Selectivity of the butadiene-1,3 hydrogenation *versus* concentration of palladium in catalysts Pd/C.

Table 6

Specific catalytic activity of catalysts Pd/C on the selective hydrogenation of butadiene-1,3 at 100°C

Type of carbon filaments	Concentration of Pd, wt.%	Specific catalytic activity, mole/s g_{Pd}
Stack-like ≡	0.5	3.1×10^{-2}
Coaxial-conic <<<<	0.58	3.7×10^{-2}
Coaxial-cylinder ||	0.60	4.0×10^{-2}

the Russian Fund of Fundamental Investigations, Grants No 00-03-32431 and SS-2120.2003.3.

Conclusions

In the reaction of selective hydrogenation of 1,3-butadiene into butylenes, the relation between activity and selectivity of the Pd/C catalysts is as follows:

- selectivity increases as dispersity of palladium increases in the filamentous carbon samples of a similar type.
- a strong interaction of palladium with prismatic graphite edges provides stabilization of Pd^{2+} in the ionic state. As the Pd^{2+} fraction in the catalyst increases, the total activity and selectivity of catalysts in the selective hydrogenation of 1,3-butadiene into butylenes decrease.

References

1. Derrien D.L., Stud.Surf.Sci.Catal., vol.27, p.613 (1986)
2. Boitiaux J.P., Cosyns J., Robert E., Appl.Catal., vol.32, No 1-2, p.145 (1987)
3. Boitiaux J.P., Cosyns J., Robert E., Appl.Catal., vol.35, No 2, p.193 (1987)
4. Hub S., Touroude R., J.Catal., vol. 114, p.411 (1988)
5. Murzin D.Yu., Khim Prom-st, No 1, p. 14 (1999).
6. Semikolenov V.A., Zh.Pr.Kh., vol. 70, vyp. 5, p. 785 (1997).
7. Semikolenov V.A., Usp. Khim., vol. 61, No 2, p. 320 (1992).
8. Zakarina N.A., Zakumbayeva G.D., High Disperse Metallic Catalysts, Nauka, Alma-Ata 1987.
9. Simonov P.A., Romanenko A.V., Prosvirin I.P., Moroz E.M., Boronin A.I., Chuvilin A.L., Likholobov V.A., Carbon, vol. 35, N 1, p.73 (1997)
10. Bertolini J.C., Delichere P., Khanra B.C., Massardier J., Noupa C., Tardy B., Catal.Lett. vol. 6, p.215 (1990)
11. Chesnokov V.V., Buyanov R.A., Usp. Khim., vol. 69, vyp. 7, p. 675 (2000).
12. Heal G.R., Mkayula L.L., Carbon, vol. 26, No 6, p.815 (1988)
13. Moulder J.F., Stickle W.F., Sobol P.E., Bomben K.D., ed. by Chastain J.. Handbook of X-Ray Photoelectron Spectroscopy, Perkin-Elmer, Eden Prairie, Minnesota, 1992.
14. Shaikhutdinov Sh.K., Zaikovskii V.I., Avdeeva L.B., Appl. Catal.A., vol.148, p.123 (1996)
15. Simonov P.A., Troitskii S.Yu., Likholobov V.A., Kinet. Katal., vol. 41, No 2, p. 281 (2000).
16. Mason M.G., Phys. Rev.B, vol. 27, p.748 (1983)
17. Kuhrt Ch., Harsdorff M., Surf. Sci., vol. 245, p.173 (1991)
18. Fritsch A., Legare P., Surf. Sci., vol. 162, p.742 (1985)
19. Bastl Z., Piibyl O., Mikusik P., Czech.J.Phys., vol. B34, p.981 (1984)
20. Vijayakrishnau V., Chainami D., Sarme D.D., Rao C.N.R., J.Phys.Chem., vol. 96, p.8679 (1992)

Received 25 October 2002.